

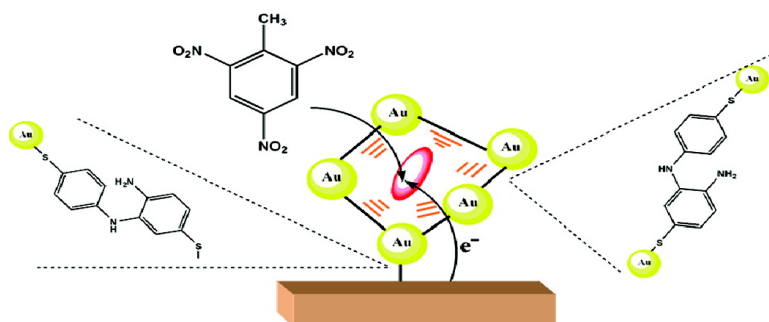
Article

# Imprinting of Molecular Recognition Sites through Electropolymerization of Functionalized Au Nanoparticles: Development of an Electrochemical TNT Sensor Based on #-Donor#Acceptor Interactions

Michael Riskin, Ran Tel-Vered, Tatyana Bourenko, Eran Granot, and Itamar Willner

*J. Am. Chem. Soc.*, **2008**, 130 (30), 9726-9733 • DOI: 10.1021/ja711278c • Publication Date (Web): 03 July 2008

Downloaded from <http://pubs.acs.org> on February 8, 2009



## More About This Article

Additional resources and features associated with this article are available within the HTML version:

- Supporting Information
- Links to the 4 articles that cite this article, as of the time of this article download
- Access to high resolution figures
- Links to articles and content related to this article
- Copyright permission to reproduce figures and/or text from this article

[View the Full Text HTML](#)

## Imprinting of Molecular Recognition Sites through Electropolymerization of Functionalized Au Nanoparticles: Development of an Electrochemical TNT Sensor Based on $\pi$ -Donor–Acceptor Interactions

Michael Riskin, Ran Tel-Vered, Tatyana Bourenko, Eran Granot, and Itamar Willner\*

*Institute of Chemistry, Center for Nanoscience, The Hebrew University of Jerusalem, Jerusalem 91904, Israel*

Received December 20, 2007; E-mail: willnea@vms.huji.ac.il

**Abstract:** Electrochemical sensors for the analysis of TNT with enhanced sensitivities are described. The enhanced sensitivities are achieved by tailoring  $\pi$ -donor–acceptor interactions between TNT and  $\pi$ -donor-modified electrodes or  $\pi$ -donor-cross-linked Au nanoparticles linked to the electrode. In one configuration a *p*-aminothiophenolate monolayer-modified electrode leads to the analysis of TNT with a sensitivity corresponding to 17 ppb (74 nM). In the second configuration, the cross-linking of Au NPs by oligothioaniline bridges to the electrode yields a functionalized electrode that detects TNT with a sensitivity that corresponds to 460 ppt (2 nM). Most impressively, the imprinting of molecular TNT recognition sites into the  $\pi$ -donor oligoaniline-cross-linked Au nanoparticles yields a functionalized electrode with a sensitivity that corresponds to 46 ppt (200 pM). The electrode reveals high selectivity, reusability, and stability.

### Introduction

Sensors for the detection of explosives are important for various disciplines including humanitarian demining,<sup>1</sup> remediation of explosives waste sites, homeland security, and forensic applications.<sup>2</sup> Different sensors for analyzing explosives and, specifically, nitrobenzene (or nitrotoluene) derivatives were reported in the past decade.<sup>3</sup> These included optical sensors where the fluorescence of functional polymers was quenched by the nitroaromatic compounds,<sup>4,5</sup> luminescent polymer nanoparticles, such as polysilole, that were quenched by trinitrotoluene (TNT),<sup>6</sup> or fluorescent silicon nanoparticles that were quenched by nitroaromatic vapors.<sup>7</sup>

The redox activity of the nitro groups associated with many of the explosives was used to develop electrochemical sensors,<sup>8</sup>

and modified electrodes such as mesoporous SiO<sub>2</sub>-functionalized electrodes were employed to enhance the sensitivity of detection of nitroaromatic explosives.<sup>9</sup> Other electronic devices for the analysis of explosives included surface acoustic wave (SAW) systems. The coating of the piezoelectric devices with silicon polymers,<sup>10</sup> carbowax<sup>11</sup> or cyclodextrin polymers<sup>12</sup> yielded functional coatings that enabled the electronic transduction of explosives adsorbed to these matrices. The eliciting of antibodies that exhibit specific binding to nitroaromatics enabled the development of biosensors for explosives, using immunocomplexes as sensing units. This was exemplified with the development of TNT biosensors based on the displacement of the anti-TNT antibody from a surface-confined immunocomplex by TNT and the transduction of the dissociation of the antibody by surface plasmon resonance (SPR) spectroscopy<sup>13,14</sup> or quartz crystal microbalance (QCM) measurements.<sup>15</sup> Also, a quantum dot-based fluorescent biosensor was developed by the application of antibody-functionalized quantum dots as reporter units. The association of a quencher–TNT conjugate to the antibody resulted in the FRET quenching of the quantum dots, and the displacement of the conjugate by TNT regenerated the fluorescence of the quantum dots.<sup>15</sup> Although substantial progress was achieved in the sensing of explosives, the different analytical

- (1) Rouhi, A. M. *Chem. Eng. News* **1997**, 75 (10), 14–22.
- (2) Smith, K. D.; McCord, B. R.; MacCrehan, W. A.; Mount, K.; Rowe, W. F. *J. Forensic. Sci.* **1999**, 44, 789–794.
- (3) Toal, S. J.; Trogler, W. C. *J. Mater. Chem.* **2006**, 16, 2871–2883.
- (4) (a) Swager, T. M. *Acc. Chem. Res.* **1998**, 31, 201–207. (b) McQuade, D. T.; Pullen, A. E.; Swager, T. M. *Chem. Rev.* **2000**, 100, 2537–2574. (c) Yang, J.-S.; Swager, T. M. *J. Am. Chem. Soc.* **1998**, 120, 11864–11873.
- (5) (a) Chang, C.-P.; Chao, C.-Y.; Huang, J.-H.; Li, A.-K.; Hsu, C.-S.; Lin, M.-S.; Hsieh, B.-R.; Su, A.-C. *Synth. Met.* **2004**, 144, 297–301. (b) Sohn, H.; Sailor, M. J.; Magde, D.; Trogler, W. C. *J. Am. Chem. Soc.* **2003**, 125, 3821–3830.
- (6) (a) Chen, J.; Law, C. C. W.; Lam, J. W. Y.; Dong, Y.; Lo, S. M. F.; Williams, I. D.; Zhu, D.; Tang, B. Z. *Chem. Mater.* **2003**, 15, 1535–1546. (b) Toal, S. J.; Magde, D.; Trogler, W. C. *Chem. Commun.* **2005**, 5465–5467.
- (7) Content, S.; Trogler, W. C.; Sailor, M. J. *Chem.—Eur. J.* **2000**, 6, 2205–2213.
- (8) (a) Wang, J.; Bhada, R. K.; Lu, J.; MacDonald, D. *Anal. Chim. Acta* **1998**, 361, 85–91. (b) Wang, J.; Hocesvar, S. B.; Ogorevc, B. *Electrochem. Commun.* **2004**, 6, 176–179. (c) Hrapovic, S.; Majid, E.; Liu, Y.; Male, K.; Luong, J. H. T. *Anal. Chem.* **2006**, 78, 5504–5512. (d) Zhang, H.-X.; Hu, J.-S.; Yan, C.-J.; Jiang, L.; Wan, L.-J. *Phys. Chem. Chem. Phys.* **2006**, 8, 3567–3572.

- (9) Zhang, H.-X.; Cao, A.-M.; Hu, J.-S.; Wan, L.-J.; Lee, S.-T. *Anal. Chem.* **2006**, 78, 1967–1971.
- (10) McGill, R. A.; Mlsna, T. E.; Chung, R.; Nguyen, V. K.; Stepnowski, J. *Sens. Actuators, B* **2000**, 65, 5–9.
- (11) Kannan, G. K.; Nimal, A. T.; Mittal, U.; Yadava, R. D. S.; Kapoor, J. C. *Sens. Actuators, B* **2004**, 101, 328–334.
- (12) Yang, X.; Du, X. X.; Shi, J.; Swanson, B. *Talanta* **2001**, 54, 439–445.
- (13) Larsson, A.; Angbrant, J.; Ekeröth, J.; Mansson, P.; Liedberg, B. *Sens. Actuators, B* **2006**, 113, 730–748.
- (14) Shankaran, D. R.; Gobi, K. V.; Sakai, T.; Matsumoto, K.; Toko, K.; Miura, N. *Biosens. Bioelectron.* **2005**, 20, 1750–1756.

protocols suffer from insufficient sensitivity, lack of specificity, long analysis time intervals, and/or complex and expensive analytical protocols.

The unique electronic and optical properties of metallic and semiconductor nanoparticles, NPs, added new dimensions to the area of sensors. The aggregation of Au NPs as a result of sensing events and the formation of an interparticle coupled plasmon absorbance was used for the development of colorimetric sensors.<sup>16</sup> For example, the color changes as a result of the aggregation of Au nanoparticles were used to detect phosphatase activity,<sup>17</sup> polynucleotides,<sup>18</sup> or alkali (lithium)<sup>19</sup> ions. Also, the shifts in the plasmonic absorption bands associated with Au nanoclusters as a result of changes in the surface dielectric properties upon sensing were used to develop optical sensors for dopamine,<sup>20</sup> adrenaline,<sup>21</sup> cholesterol,<sup>22</sup> DNA hybridization,<sup>23</sup> and pH changes.<sup>24</sup> The layer-by-layer deposition of Au NPs on electrodes by the electrostatic cross-linking of the NPs by charged molecular receptors was used to construct electrochemical sensors for different neurotransmitters.<sup>25</sup> Here we wish to report on a novel approach to design functionalized Au-NP electrodes for the sensitive electrochemical analysis of trinitrotoluene, TNT (**1**). The electrodes are constructed by the electropolymerization of thioaniline-capped Au NPs on the electrodes. The oligoaniline units that bridge the Au NPs act as  $\pi$ -donor sites that concentrate TNT at the electrode surface, while the Au NPs provide three-dimensional conductivity for the electrochemical detection of TNT. Specifically, we demonstrate a novel method to generate selective molecular recognition sites on electrodes by the electropolymerization of functionalized Au NPs. This is exemplified with the generation of recognition sites for TNT in the electropolymerized oligoaniline-cross-linked Au NPs aggregates. The imprinting procedure increases, together with the complementary  $\pi$ -donor–acceptor interactions, the association of TNT to the sensing electrode, thereby enhancing the sensitivity of the analysis, and it results in a highly selective TNT-detection electrode.

The imprinting of molecular recognition in organic or inorganic polymer matrices is a common practice to generate selective binding sites for the imprinted substrates.<sup>26</sup> Indeed, numerous optical<sup>27</sup> or electronic<sup>28</sup> sensors based on imprinted

polymer matrices were developed in the past two decades. For example, electrochemical sensors that consisted of imprinted organic<sup>29</sup> or inorganic<sup>30</sup> polymers were developed, and imprinted inorganic matrices associated with the gate surface of field-effect transistors were applied for the stereoselective or chiroselective analysis of the imprinted substrates.<sup>31</sup> Similarly, a quartz crystal microbalance<sup>32</sup> and surface plasmon resonance spectroscopy<sup>33</sup> were used as readout methods for the binding of substrates to the imprinted sites. The use of imprinted polymers as functional sensing matrices suffers, however, from several basic limitations. The density of imprinted sites is relatively low, and thus, for sensitive sensing thick polymer matrices are required. This leads, however, to slow binding of the analytes to the recognition sites (long analysis time intervals) and to inefficient communication between the binding sites and the transducers. In fact, several studies suggested the use of imprinted monolayers,<sup>34</sup> multilayers,<sup>35</sup> and thin films to overcome these difficulties. In the present study we introduce a new method for imprinting of molecular recognition sites that is based on the electropolymerization of functional Au NPs on electrodes.

## Experimental Section

Au nanoparticles functionalized with 2-mercaptoethane sulfonic acid and *p*-aminothiophenol (Au NPs) were prepared by mixing a 10 mL solution containing 197 mg of HAuCl<sub>4</sub> in ethanol and a 5 mL solution containing 42 mg of mercaptoethane sulfonate and 8 mg of *p*-aminothiophenol in methanol. The two solutions were stirred in the presence of 2.5 mL of glacial acetic acid in an ice bath for 1 h. Subsequently, 7.5 mL of aqueous solution of 1 M sodium borohydride, NaBH<sub>4</sub>, was added dropwise, resulting in a

- (15) Goldman, E. R.; Medintz, I. L.; Whitley, I. L.; Hayhurst, A.; Clapp, A. R.; Uyeda, H. T.; Deschamps, J. R.; Lassman, M. E.; Mattoussi, H. *J. Am. Chem. Soc.* **2005**, *127*, 6744–6751.
- (16) (a) Daniel, M.-C.; Astruc, D. *Chem. Rev.* **2004**, *104*, 293–346. (b) Rosi, N. L.; Mirkin, C. A. *Chem. Rev.* **2005**, *105*, 1547–1562.
- (17) Choi, Y.; Ho, N.-H.; Tung, C.-H. *Angew. Chem., Int. Ed.* **2007**, *46*, 707–709.
- (18) Storhoff, J. J.; Elghanian, R.; Mucic, R. C.; Mirkin, C. A.; Letsinger, R. L. *J. Am. Chem. Soc.* **1998**, *120*, 1959–1964.
- (19) Obare, S. O.; Hollowell, R. E.; Murphy, C. J. *Langmuir* **2002**, *18*, 10407–10410.
- (20) Matsui, J.; Akamatsu, K.; Hara, N.; Miyoshi, D.; Nawafune, H.; Tamaki, K.; Sugimoto, N. *Anal. Chem.* **2005**, *77*, 4282–4285.
- (21) Matsui, J.; Akamatsu, K.; Nishiguchi, S.; Miyoshi, D.; Nawafune, H.; Tamaki, K.; Sugimoto, N. *Anal. Chem.* **2004**, *76*, 1310–1315.
- (22) Tokareva, I.; Tokarev, I.; Minko, S.; Hutter, E.; Fendler, J. H. *Chem. Commun.* **2006**, *31*, 3343–3345.
- (23) Hu, W. P.; Chen, S.-J.; Huang, K.-T.; Hsu, J. H.; Chen, W. Y.; Chang, G. L.; Lai, K.-A. *Biosens. Bioelectron.* **2004**, *19*, 1465–1471.
- (24) Jiang, G.; Baba, A.; Ikarashi, H.; Xu, R.; Locklin, J.; Kashif, K. R.; Shinbo, K.; Kato, K.; Kaneko, F.; Advincula, R. *J. Phys. Chem. C* **2007**, *111*, 18687–18694.
- (25) (a) Shipway, A. N.; Lahav, M.; Willner, I. *Adv. Mater.* **2000**, *12*, 993–998. (b) Lahav, M.; Gabai, R.; Shipway, A. N.; Willner, I. *Chem. Commun.* **1999**, *19*, 1937–1938. (c) Shipway, A. N.; Lahav, M.; Blonder, R.; Willner, I. *Chem. Mater.* **1999**, *11*, 13–15. (d) Lahav, M.; Shipway, A. N.; Willner, I.; Nielsen, M. B.; Stoddart, J. F. *J. Electroanal. Chem.* **2000**, *482*, 217–221.
- (26) (a) Wulff, G. *Angew. Chem., Int. Ed.* **1995**, *34*, 1812–1832. (b) Wulff, G. *Chem. Rev.* **2002**, *102*, 1–27. (c) Mosbach, K. *Trends Biochem. Sci.* **1994**, *19*, 9–14. (d) Haupt, K.; Mosbach, K. *Chem. Rev.* **2000**, *100*, 2495–2504. (e) Bossi, A.; Bonini, F.; Turner, A. P. F.; Piletsky, S. A. *Biosens. Bioelectron.* **2007**, *22*, 1131–1137.
- (27) (a) Suarez-Rodriguez, J. L.; Diaz-Garcia, M. E. *Biosens. Bioelectron.* **2001**, *16*, 955–961. (b) Surugiu, I.; Svitel, J.; Ye, L.; Haupt, K.; Danielsson, B. *Anal. Chem.* **2001**, *73*, 4388–4392. (c) Wang, W.; Gao, S.; Wang, B. *Org. Lett.* **1999**, *1*, 1209–1212. (d) Hu, X.; An, Q.; Li, G.; Tao, S.; Liu, J. *Angew. Chem., Int. Ed.* **2006**, *45*, 8145–8148.
- (28) (a) Liang, H.-J.; Ling, T.-R.; Rick, J. F.; Chou, T.-C. *Anal. Chim. Acta* **2005**, *542*, 83–89. (b) Kirsch, N.; Hart, J. P.; Bird, D. J.; Luxton, R. W.; McCalley, D. V. *Analyst* **2001**, *126*, 1936–1941.
- (29) (a) Weng, C.-H.; Yeh, W.-M.; Ho, K.-C.; Lee, G.-B. *Sens. Actuators, B* **2007**, *B121*, 576–582. (b) Shoji, R.; Takeuchi, T.; Kubo, I. *Anal. Chem.* **2003**, *75*, 4882–4886.
- (30) (a) Zhou, Y.; Yu, B.; Shiu, E.; Levon, K. *Anal. Chem.* **2004**, *76*, 2689–2693. (b) Fireman-Shoresh, S.; Turyan, I.; Mandler, D.; Avnir, D.; Marx, S. *Langmuir* **2005**, *21*, 7842–7847. (c) Lahav, M.; Kharitonov, A. B.; Katz, O.; Kunitake, T.; Willner, I. *Anal. Chem.* **2001**, *73*, 720–723.
- (31) (a) Zayats, M.; Lahav, M.; Kharitonov, A. B.; Willner, I. *Tetrahedron* **2002**, *58*, 815–824. (b) Pogorelova, S. P.; Zayats, M.; Bourenko, T.; Kharitonov, A. B.; Lioubashevski, O.; Katz, E.; Willner, I. *Anal. Chem.* **2003**, *75*, 509–517.
- (32) (a) Pogorelova, S. P.; Bourenko, T.; Kharitonov, A. B.; Willner, I. *Analyst* **2002**, *127*, 1484–1491. (b) Cao, L.; Li, S. F. Y.; Zhou, X. C. *Analyst* **2001**, *126*, 184–188.
- (33) (a) Matsunaga, T.; Hishiya, T.; Takeuchi, T. *Anal. Chim. Acta* **2007**, *591*, 63–67. (b) Li, X.; Husson, S. M. *Biosens. Bioelectron.* **2006**, *22*, 336–348. (c) Raitman, O. A.; Chegel, V. I.; Kharitonov, A. B.; Zayats, M.; Katz, E.; Willner, I. *Anal. Chim. Acta* **2004**, *504*, 101–111.
- (34) (a) Lahav, M.; Katz, E.; Doron, A.; Patolsky, F.; Willner, I. *J. Am. Chem. Soc.* **1999**, *121*, 862–863. (b) Lahav, M.; Katz, E.; Willner, I. *Langmuir* **2001**, *17*, 7387–7395. (c) Mirsky, V. M.; Hirsch, T.; Piletsky, S. A.; Wolfbeis, O. S. *Angew. Chem., Int. Ed.* **1999**, *38*, 1108–1110. (d) Li, X.; Husson, S. M. *Langmuir* **2006**, *22*, 9658–9663.
- (35) (a) Shi, F.; Liu, Z.; Wu, G.; Zhang, M.; Chen, H.; Wang, Z.; Zhang, X.; Willner, I. *Adv. Funct. Mater.* **2007**, *17*, 1821–1827. (b) Panasyuk, T. L.; Mirsky, V. M.; Piletsky, S. A.; Wolfbeis, O. S. *Anal. Chem.* **1999**, *71*, 4609–4613.

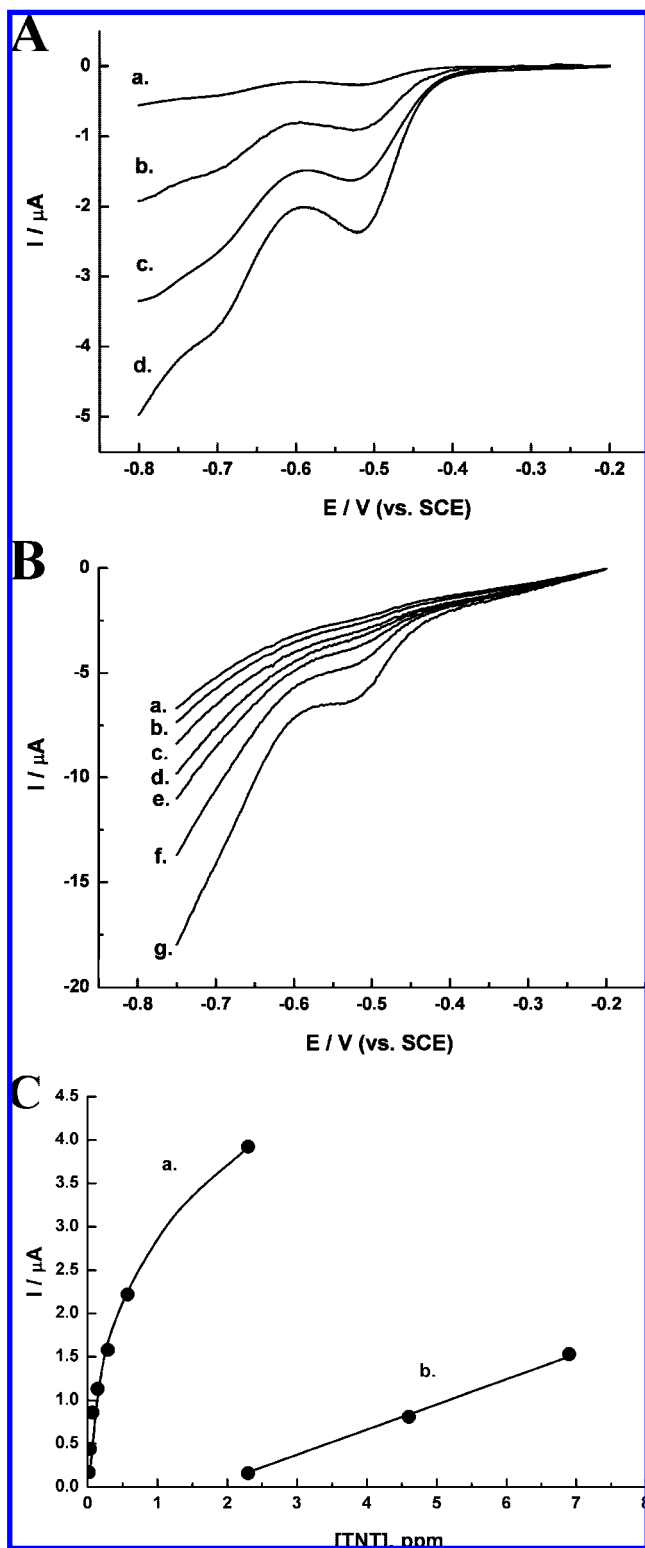


**Figure 1.** (A) Linear sweep voltammograms corresponding to the reduction of (a) 2.3, (b) 4.6, (c) 6.9, and (d) 9.2 ppm TNT in PB at a bare Au electrode. Scan rate is  $20 \text{ mV s}^{-1}$ . The scan direction is from positive to negative. (B) Linear sweep voltammograms corresponding to the reduction of (a) 17 ppb; (b) 34 ppb; (c) 72, (d) 144, (e) 288, (f) 575, and (g) 2300 ppb TNT in PB at a *p*-aminothiophenol-functionalized Au electrode. Scan rate is  $20 \text{ mV s}^{-1}$ . The scan direction is from positive to negative. (C) Calibration curves corresponding to the analysis of TNT at the (a) *p*-aminothiophenol-functionalized Au electrode and (b) bare Au electrode. All data were recorded after interacting the respective electrodes with the TNT solution sample for a time interval of 50 s. All of the experiments were performed under an inert Ar atmosphere.

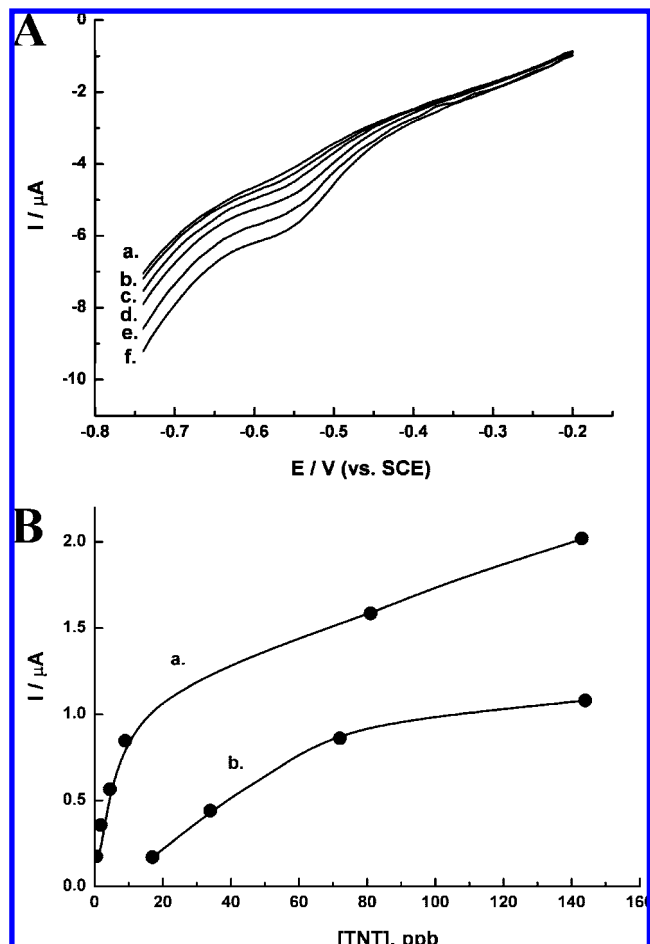


**Figure 2.** (A) Linear sweep voltammograms corresponding to the reduction of (a) 0.46, (b) 1.8, (c) 4.5, (d) 9, (e) 81, and (f) 143 ppb TNT in PB on an oligoaniline-cross-linked Au NPs-functionalized electrode. Scan rate is  $20 \text{ mV s}^{-1}$ . The scan direction is from positive to negative. (B) Calibration curves corresponding to the analysis of TNT at the (a) oligoaniline-cross-linked Au NPs-functionalized electrode and (b) *p*-aminothiophenol-functionalized Au electrode. All data were recorded after interacting the respective electrodes with the TNT solution sample for a time interval of 50 s. All of the experiments were performed under an inert Ar atmosphere.

dark color solution associated with the presence of the Au NPs. The solution was stirred for 1 additional hour in an ice bath and then for 14 h at room temperature. The particles were successively washed and centrifuged (twice in each solvent) with methanol, ethanol, and diethyl ether. An average particle size of 3.5 nm was estimated using TEM (see Supporting Information, Figure S1).

Nanopure (Barnstead) ultrapure water was used in the preparation of the different solutions. Au-coated glass plates (Evaporated Coatings, PA, USA) were used as working electrodes. Prior to modification, the Au surface was flame-annealed for 5 min in an *n*-butane flame and was allowed to cool down for 10 min under a stream of Ar. Cyclic voltammetry experiments were carried out using a PC-controlled (Autolab GPES software) electrochemical analyzer potentiostat/galvanostat ( $\mu\text{Autolab}$ , type III). A graphite rod ( $d = 5 \text{ mm}$ ) was used as a counter electrode, and the reference was a saturated calomel electrode (SCE).

**Chemical Modification of the Electrodes.** *p*-Aminothiophenol-functionalized electrodes were prepared by immersing the Au plates for 24 h into a *p*-aminothiophenol ethanolic solution, 50 mM. In order to prepare the oligoaniline Au-NPs film on the electrode, the surface-tethered *p*-aminothiophenol groups were electropolymerized in the presence of the *p*-aminothiophenol-functionalized Au NPs in an electrolyte solution of 0.1 M phosphate buffer (PB) pH =

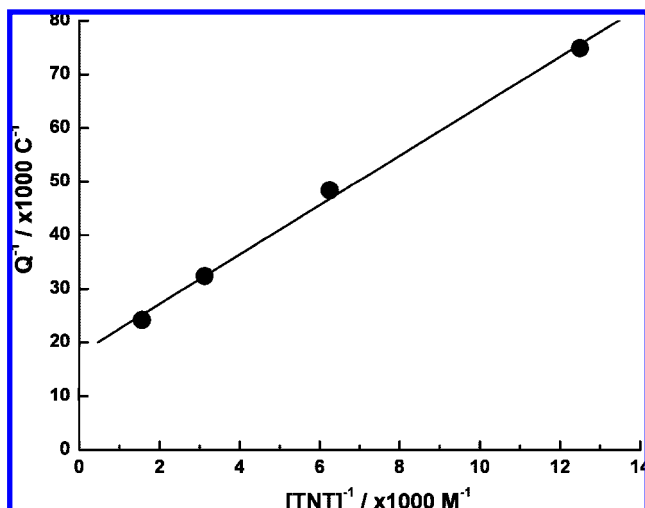


**Figure 3.** Coulometric analysis of the TNT associated with the oligoaniline-cross-linked Au NPs-functionalized electrode upon interaction of the electrode with different bulk concentrations of TNT. The functionalized electrode was immersed in the different solutions of TNT for 2 h.

7.4 that contained  $1 \text{ mg} \cdot \text{mL}^{-1}$  of the NPs. The polymerization was performed by the application of six potential cycles between  $-0.35$  and  $0.5 \text{ V}$ , at a potential scan rate of  $100 \text{ mV s}^{-1}$ . The cyclic voltammograms of the oligoaniline-bridged Au NPs associated with the Au electrode are shown in the Supporting Information, Figure S2.<sup>36</sup> The resulting films were washed with the background electrolyte solution to exclude any residual monomer from the electrode. Similarly, picric acid imprinted oligoaniline films were prepared by adding  $1 \text{ mg} \cdot \text{mL}^{-1}$  picric acid to the Au NPs mixture prior to the electropolymerization process. The extraction of the picric acid from the film was carried out by immersing the electrodes in a  $0.1 \text{ M}$  phosphate buffer solution,  $\text{pH} = 7.4$  for 2 h at room temperature under continuous agitation. The full removal of picric acid from the electropolymerized film was verified electrochemically. Prior to the sensing experiments, the PB solutions were loaded with the analytes and purged for 5 min with  $\text{N}_2$ . The current values for analyzing TNT in the different systems were derived by subtracting the current generated by the pure buffer solution from the peak current of the voltammetric wave at ca.  $-0.5 \text{ V}$  vs SCE.

## Results and Discussion

Nitrobenzene units undergo stepwise reduction to hydroxylamine groups,<sup>37</sup> according to eq 1. Figure 1A depicts the linear sweep voltammograms of TNT at a bare Au electrode. The lowest level of TNT that is detectable at the bare Au electrode is  $2.3 \text{ ppm}$  ( $10 \mu\text{M}$ ). The aim of the present study is to enhance the sensitivity of TNT analysis by modifying the electrode surface with  $\pi$ -donor groups that would concentrate the TNT analyte at the electrode surface by  $\pi$ -donor–acceptor interactions. Thus, the Au surface was modified with *p*-aminothiophenol (**2**) that acts as a  $\pi$ -donor, Scheme 1A. Figure 1B shows the cyclic voltammograms of variable concentrations of TNT at the **2**-functionalized Au electrode. The amperometric responses of the electrode are observed at substantially lower bulk concentrations of TNT, as compared to the bare Au electrode. Figure 1C shows the derived calibration curves that correspond to the analysis of TNT at the **2**-modified electrode, curve (a),

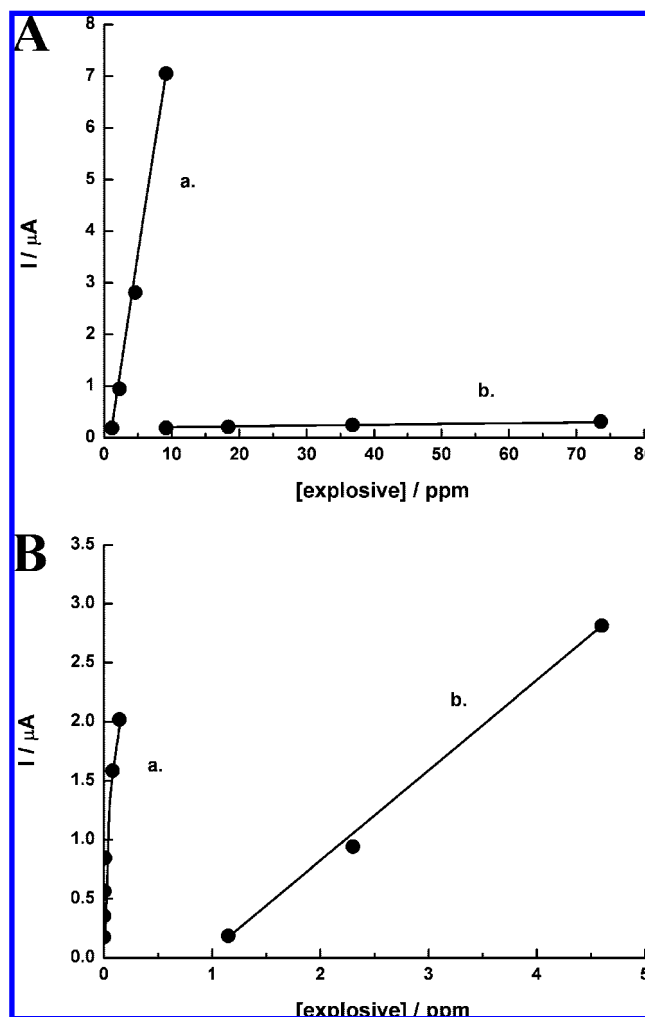
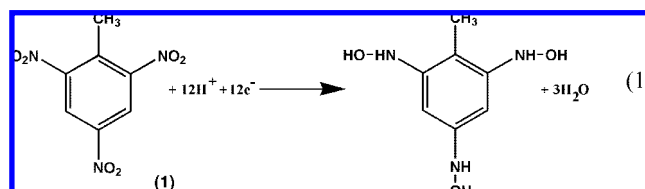


**Figure 4.** (A) Calibration curves corresponding to the analysis of (a) 2,4-DNT and (b) 4-NT at the oligoaniline-cross-linked Au NPs-functionalized electrode. (B) Calibration curves corresponding to the analysis of (a) TNT and (b) 2,4-DNT at the oligoaniline-cross-linked Au NPs-functionalized electrode. All data were recorded after interacting the respective electrodes with the TNT solution sample for a time interval of 50 s. All of the experiments were performed under an inert Ar atmosphere.

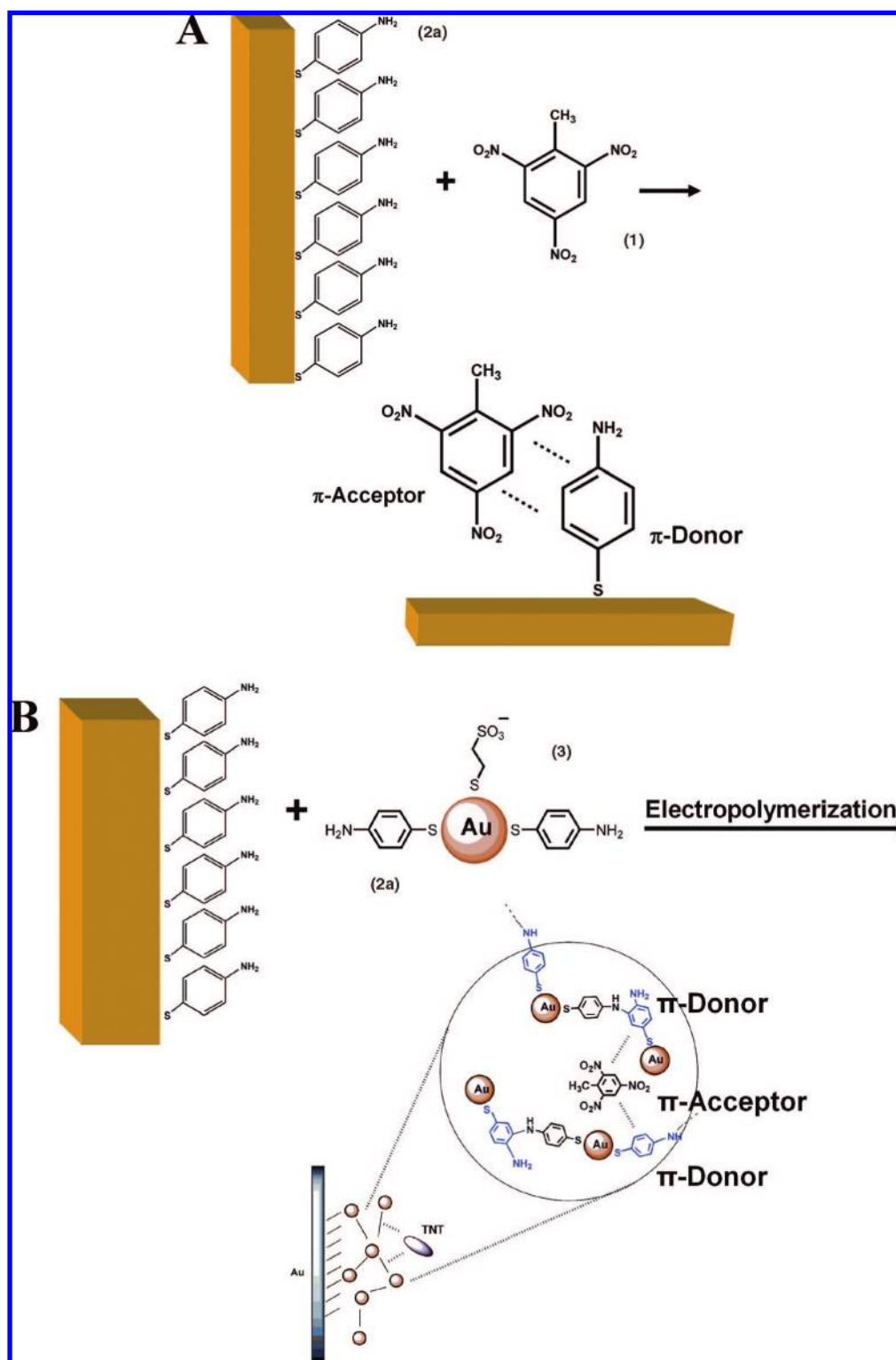
and at the bare Au surface, curve (b). The TNT can be detected at the (**2**)-functionalized surface with a sensitivity that corresponds to  $17 \text{ ppb}$  ( $74 \text{ nM}$ ). The 135-fold increase in the sensitivity for analyzing TNT by the **2**-functionalized electrode is attributed to the concentration of the analyte at the electrode surface by  $\pi$  donor–acceptor interactions with the monolayer modifier.



To further enhance the sensitivity of the detection of TNT, we decided to employ *p*-aminothiophenol-functionalized Au nanoparticles (NPs) as comodifier of the Au electrode, Scheme 1(B). Au NPs,  $3.5 \text{ nm}$  in diameter, were prepared by the sodium borohydride reduction method, and the particles were modified with a mixed capping monolayer consisting of polymerizable

(36) Granot, E.; Patolsky, F.; Willner, I. *J. Phys. Chem. B* **2004**, *108*, 5875–5881.

(37) (a) Bratin, K.; Kissinger, P. T. *Anal. Chim. Acta* **1981**, *130*, 295–311. (b) Zuman, P.; Fijalek, Z. *J. Electroanal. Chem.* **1990**, *296*, 589–593.

Scheme 1<sup>a</sup>

<sup>a</sup> (A) Analysis of TNT at a  $\pi$ -donor (*p*-aminothiophenol)-functionalized Au electrode. (B) Analysis of TNT by an oligoaniline-crosslinked Au NPs-functionalized electrode.

*p*-aminothiophenolate (**2a**) and 2-mercaptoethane sulfonic acid (**3**). The latter component enhances the solubility of the NPs in the aqueous medium. The functionalized Au NPs were then electropolymerized in the presence of the **2a**-functionalized Au electrode to yield the oligoaniline  $\pi$ -donor-bridged Au NP aggregates on the electrode surface. We anticipate enhanced sensitivity for analyzing TNT at the resulting Au NP-function-

alized electrode due to two complementary effects: (i) The content of the  $\pi$ -donor oligoaniline units increases as a result of the formation of Au NP aggregates. (ii) the Au NPs provide a conductive roughened array, and thus, electrochemical analysis of TNT is feasible at a roughened surface with a higher content of  $\pi$ -donor sites for the given concentration of the analyte. Figure 2A shows the linear sweep voltammograms observed

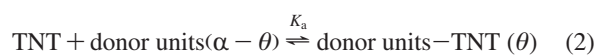
**Table 1.** Analysis of TNT in Aqueous Media by Different Sensor Systems

method	detection limit	reference
imprinted electropolymerized oligoaniline-cross-linked Au NPs	46 ppt	–
electrochemical determination by metallic nanoparticle-carbon nanotube composites	1 ppb	8c
electrochemical detection by carbon nanotubes	5 ppb	8d
electrochemical detection by mesoporous SiO <sub>2</sub> -modified electrodes	414 ppt	9
luminescent oligo(tetraphenyl)silole nanoparticles as chemical sensors	20 ppb	6b
remote microelectrode electrochemical sensor in water	50 ppb	8a
adsorptive stripping detection by carbon nanotube-modified GCE	600 ppt	8b
biochip (on gold) QCM detection	1–10 ppb	13
biochip (on gold) SPR detection	1 ppb	13
SPR immunosensor detection	90 ppt	14

upon analyzing variable concentrations of TNT by the Au NPs-functionalized electrode. Figure 2B, curve (a) shows the derived calibration curve. By applying the electrochemically aggregated  $\pi$ -donor Au NPs electrode, the TNT is sensed with a detection limit that corresponds to 460 ppt (2 nM). For comparison, Figure 2B, curve (b) depicts the calibration curve for analyzing TNT by the **2a**-monolayer-functionalized electrode. The amperometric responses in the presence of the Au NP-modified electrode, in the lower concentration range of TNT, are substantially higher, and the sensitivity is improved by a factor of 37 compared with the monolayer configuration. The sensitivity observed with the Au NP-modified electrode is already impressive, and hence we decided to structurally and functionally characterize this electrode.

The covalent binding of the Au NP bridged to the electrode was followed by quartz crystal microbalance experiments. Upon the electropolymerization of the **2a**-functionalized Au NPs onto the Au/quartz crystal, a frequency decrease that corresponded to 300 Hz was observed. This value translates to a surface coverage of the particles that corresponds to ca.  $3 \times 10^{12}$  Au NPs  $\cdot$  cm<sup>-2</sup>.

The association constant of TNT to the oligoaniline  $\pi$ -donor bridging units associated with the Au NPs, eq 2, was determined electrochemically. The association constant is given by eq 3, where  $\alpha$  is the number of  $\pi$ -donor sites in the system and  $\theta$  is the fraction of sites that is complexed by TNT at any bulk concentration of the analyte. Equation 3 can be rewritten in the form of eq 3a, and the value of  $\theta$  is derived from the coulometric analysis of the first wave of reduction of TNT at any bulk concentration of TNT. The charge associated with the bound TNT is proportional to the number of occupied  $\pi$ -donor sites. Figure 3 shows the analysis of the association constant of TNT to the binding sites according to eq 3a. The derived association constant corresponds to  $K_a = 3100 \pm 50$  M<sup>-1</sup>. It should be noted that this method for deriving the association constants assumes that the binding of TNT to the  $\pi$ -donor sites is unaffected by neighboring occupied sites. At the low concentrations of TNT at which the association constant was derived, this assumption is justified.

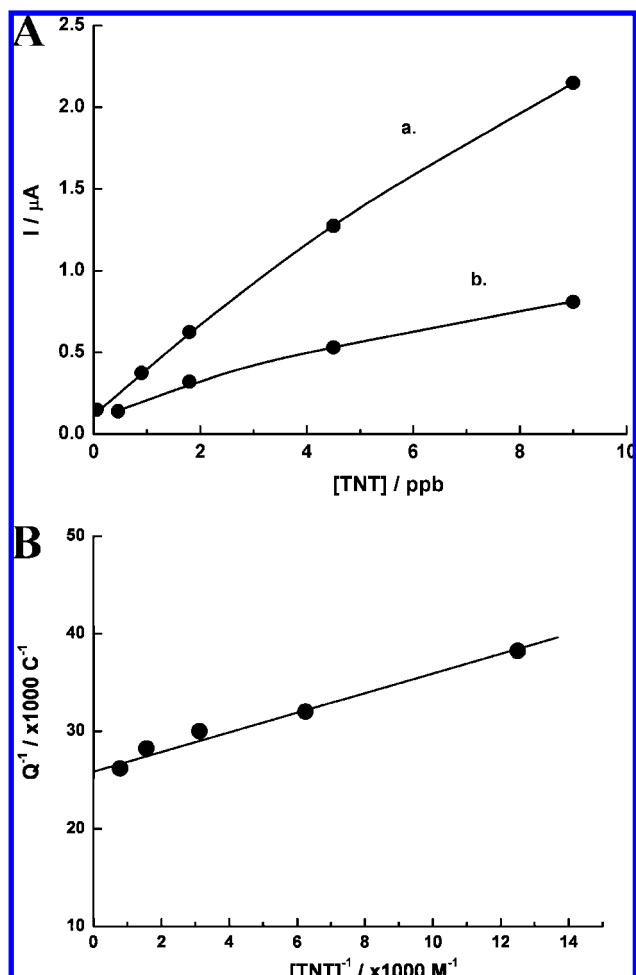


$$K_a = \frac{\theta}{(\alpha - \theta)[\text{TNT}]} \quad \text{or,} \quad (3)$$

$$\frac{1}{\theta} = \frac{1}{\alpha} + \frac{1}{\alpha \cdot K_a [\text{TNT}]} \quad (3a)$$

An important aspect of the Au NPs-functionalized electrodes relates to their specificity toward detecting different nitrotoluene explosives. Accordingly, the sensing of 2,4-dinitrotoluene, DNT (**4**), and of 4-nitrotoluene, NT (**5**), by the Au NPs-functionalized electrode was examined. Figure 4A, curves (a) and (b), depicts the resulting calibration curves. The detection limits for analyzing DNT and NT correspond to 1.1 ppm (5  $\mu$ M) and 9.2 ppm (40  $\mu$ M), respectively. Evidently, these values are  $2.6 \times 10^3$ -fold and  $2.0 \times 10^4$ -fold lower than the sensitivity for the detection of TNT. These results are consistent with the fact that DNT and NT exhibit lower  $\pi$ -acceptor properties due to the decreased number of the electron-withdrawing nitro groups, and hence their concentration at the electrode surface via  $\pi$ -donor–acceptor interactions is substantially lower. It is therefore expected that the sensitivities for the detection of the nitroaromatic substrates decrease as the  $\pi$ -acceptor properties of the analytes are lowered. Figure 4B compares the calibration curves for analyzing TNT and DNT by the Au NPs functionalized electrode. A selectivity factor of ca. 20 (corresponding to the ratio of the slopes) is derived. The Au NP-modified electrode can be recycled by extracting the analyte TNT, and it reveals an excellent stability (extraction of the bound TNT was performed by shaking the electrode in a phosphate buffer solution, pH = 7.4, for 2 h). The Au NPs-modified electrode was operated for seven days with no noticeable change in its functional activity. It should be noted that TNT and DNT reveal no selectivity upon electrochemical analysis by the same Au electrode (see Figure S3, Supporting Information). These results imply that the selectivity is, indeed, induced by the  $\pi$ -donor–acceptor interactions between the different nitroaromatic compounds and the  $\pi$ -donor oligoaniline bridges.

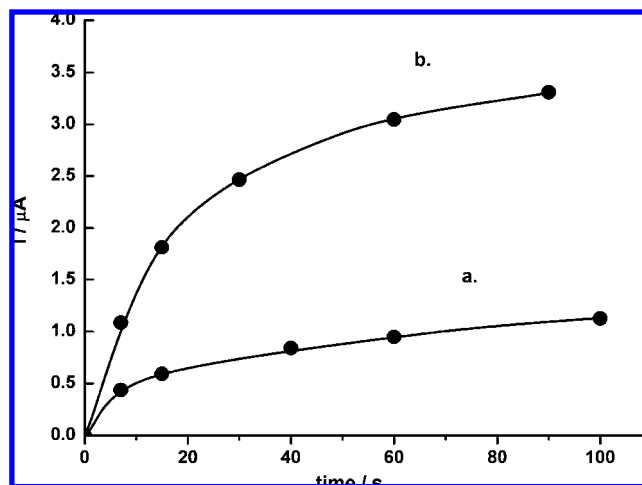
Although the Au NPs-functionalized electrode revealed an impressive sensitivity, we searched for possibilities to enhance the sensitivity (as well as the selectivity) of the electrode for analyzing TNT. This could possibly be accomplished by increasing the binding affinity of the analyzed substrate to the Au NP sensing surface. Toward this end, we realized that the imprinting of molecular recognition sites for TNT in the oligoaniline  $\pi$ -donor bridged Au NPs array associated with the electrode might provide an effective means for enhancing the sensitivity of the sensor electrode. That is, in addition to the association of TNT to the  $\pi$ -donor sites, the formation of imprinted  $\pi$ -donor molecular contours around the complex might synergistically bind the TNT analyte to the sensing surface, thus increasing the association constant. Accordingly, we used picric acid (**6**) as the imprinting substrate. The imprint molecule has three nitro groups, analogous to the analyte TNT, the OH functionality resembles the dimensions of the methyl group, and the molecule exhibits strong  $\pi$ -acceptor properties. The high solubility of **6** in water permits the effective formation of the  $\pi$ -donor acceptor complex between **6** and the **2a**-functionalized Au NPs, Scheme 2. Accordingly, the picric acid complexed **2a**-functionalized Au NPs were electropolymerized at the **2a**-modified electrode, and the imprint molecules of picric acid were then removed by extraction to yield the imprinted Au NPs-functionalized electrode, Scheme 2. The resulting electrode was then used to analyze TNT. Figure 5A, curve (a) shows the calibration curve that corresponds to the analysis of TNT by the **6**-imprinted oligoaniline-bridged Au NPs electrode. For comparison, curve (b) depicts the calibration curve observed with the nonimprinted cross-linked Au NPs electrodes. Evidently, the amperometric responses with the imprinted Au NPs electrode are substantially higher as compared to the nonimprinted electrode, within a similar concentration range of the analyte. The sensitivity



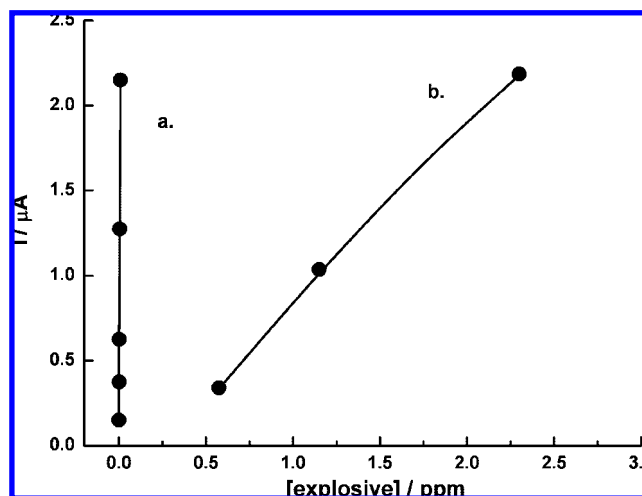
**Figure 5.** (A) Calibration curves corresponding to the analysis of TNT at the (a) picric acid imprinted oligoaniline-cross-linked Au NPs-functionalized electrode and (b) nonimprinted oligoaniline-cross-linked Au NPs-functionalized electrode. All data were recorded after interacting the respective electrodes with the TNT solution sample for a time interval of 50 s. (B) Coulometric analysis of the TNT associated to the picric acid imprinted oligoaniline-cross-linked Au NPs-functionalized electrode upon interaction of the electrode with different bulk concentrations of TNT. The functionalized electrode was immersed in the different solutions of TNT for 2 h.

for analyzing TNT by the 6-imprinted Au NPs electrode corresponds to 46 ppt (200 pM), a value that is 10-fold higher than the sensitivity with the nonimprinted Au NPs electrode (and  $5 \times 10^4$  fold higher than the initial, bare Au electrode configuration). To account for the enhanced sensitivity observed with the imprinted Au NPs array, we analyzed the association constant of TNT to the imprinted sensing surface. Figure 5B shows the coulometric analysis of the TNT bound to the imprinted Au NPs electrode, at different bulk concentrations of TNT, according to eq 3a. The derived association constant corresponded to  $(2.6 \times 10^4) \pm 600 \text{ M}^{-1}$ , a value that is ca. 8-fold higher than that with the nonimprinted oligoaniline bridged Au NPs electrode. Thus, the enhanced sensitivity for analyzing TNT by the imprinted electrode is attributed to improved concentration of the analyte at the electrode surface as a result of higher affinity of TNT to the imprinted  $\pi$ -donor sites. The imprinted oligoaniline-cross-linked Au NP-modified electrode operated for 1 week at room temperature, showing a ca. 10% decrease in the TNT signal.

Throughout the study, we interacted the sensing electrodes with the TNT samples for a time interval of 50 s, prior to the electrochemical probing of the TNT signals. This time interval was



**Figure 6.** Time-dependent electrical responses upon the analysis of an aqueous TNT sample, 0.1 mM, by the (a) nonimprinted oligoaniline-bridged Au NPs-functionalized electrode and (b) imprinted oligoaniline-bridged Au NPs-modified electrodes. In all experiments the scanned range was  $-0.4$  to  $-0.6 \text{ V}$  vs SCE. Scan rate was  $25 \text{ mV s}^{-1}$ . Experiments were performed under an inert Ar atmosphere.

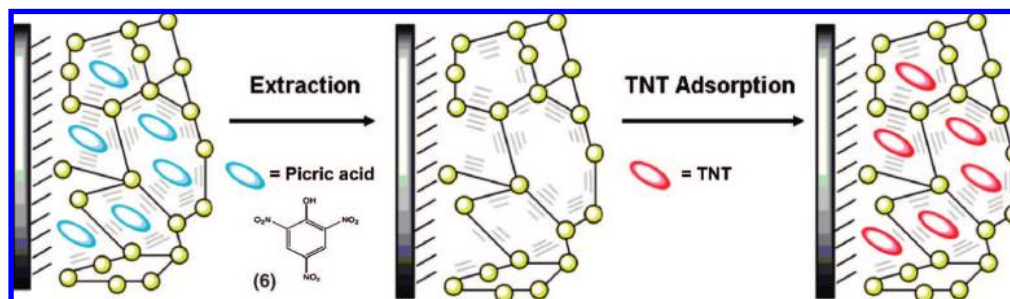


**Figure 7.** Calibration curves corresponding to the analysis of (a) TNT and (b) 2,4-DNT by the picric acid imprinted oligoaniline-cross-linked Au NPs-functionalized electrode. All data were recorded after interacting the respective electrodes with the TNT solution sample for a time interval of 50 s. All of the experiments were performed under an inert Ar atmosphere.

selected after a detailed analysis of the kinetics of TNT binding to the imprinted and nonimprinted oligoaniline-bridged aggregates, associated with the electrodes. Figure 6, curve (a) depicts the kinetics of association of TNT, 0.1  $\mu\text{M}$ , to the nonimprinted Au NPs-functionalized electrode, whereas curve (b) shows the electrical response of the imprinted, oligoaniline-bridged Au NPs-functionalized Au electrode. After ca. 50 s, the electrical response of the imprinted electrode tends to level off. We found that, within the entire concentration range for analyzing TNT, a time interval of 50 s for incubating the functionalized electrodes with the samples was sufficient for generating an electrical response corresponding to 85–95% of the saturation value. These results clearly imply that the response of our sensor device is rapid and, thus, of potential practical applicability.

Furthermore, for any practical use, the analysis of TNT in real environmental samples should be elucidated. Thus, we applied the imprinted Au NPs-functionalized electrodes for analyzing aqueous



**Scheme 2.** Imprint of Molecular Recognition Sites for TNT in an Oligoaniline-Cross-linked Au NPs Film Polymerized at the Au Electrode

groundwater and seawater samples contaminated with variable concentrations of TNT (see Figure S4, Supporting Information). The results indicated that the electrical responses of TNT in the different media showed similarity, within  $\pm 12\%$ , to the results obtained in pure buffer solution.

To complete the study, we analyzed the selectivity features of the imprinted Au NPs electrode and compared it to the selectivity pattern of the nonimprinted electrode. Figure 7, curve (a) depicts the calibration curve that corresponds to the analysis of TNT by the imprinted Au NPs electrode, whereas curve (b) shows the calibration curve that corresponds to the analysis of dinitrotoluene, DNT, at the imprinted Au NPs electrode. The selectivity factor ( $\beta_{\text{TNT}}/\beta_{\text{DNT}}$ ), where  $\beta$  is the slope of the respective calibration curve, equals 215. This selectivity factor is ca. 11-fold higher than the selectivity observed for the nonimprinted Au NPs electrode. Thus, the imprinting procedure of picric acid not only increases the sensitivity of the modified electrode but also impressively enhances its selectivity toward the analysis of TNT.

It should be noted that several previous studies used particles for the analysis of imprinted analytes. For example, imprinted core–shell silica particles were used for sensing TNT.<sup>38</sup> Similarly, imprinted photonic polymers were used for chiral recognition.<sup>39</sup> The imprinting method in the present study is, however, completely different than the reported methodologies.<sup>38,39</sup> While the previous studies used traditional imprinting procedures in organic or inorganic polymer matrices and focused on miniaturizing the polymer sizes into small beads, our imprinting approach is entirely different and may be considered as “imprinting at the nanoscale”. In our system, the functionalized Au NPs act as the “monomer units” for the electropolymerization imprinting process.

## Conclusions

We have presented a systematic study on the construction of modified electrodes for the ultrasensitive detection of TNT by electrochemical means. We showed that the modification of Au electrodes by a  $\pi$ -donor thioaniline monolayer improves the sensitivity for analyzing TNT by a factor of 135 as compared to a bare Au electrode. The electrochemical aggregation of Au NPs bridged by oligoaniline units on the Au electrode further increased the sensitivity of the modified electrode by a factor of 37 as a result of the formation of a high content of  $\pi$ -donor sites on the electrode

surface and due to the three-dimensional conductivity of the NPs matrix. Finally, the imprint of molecular recognition sites into the  $\pi$ -donor oligoaniline-cross-linked Au NPs structure further enhanced the sensitivity by a factor of 10, and TNT was analyzed with a sensitivity that corresponded to 46 ppt (200 pM). Table 1 summarizes the detection limits for analyzing TNT in aqueous media by different sensor systems. It is evident that the imprinted  $\pi$ -donor Au NPs cross-linked array presents a highly sensitive method for analyzing TNT. The closest sensor configuration with comparable sensitivity involves an immunosensor and SPR readout. The limited stability of antibodies and the long detection time intervals required by the TNT-induced displacement of the antibody from the SPR transducer highlight, however, the advantages of the present sensor system.

We should emphasize the successful imprinting of molecular recognition sites in aggregated structures of modified NPs. As far as we are aware, this represents the first attempt to use modified particles to generate imprinted molecular sites. The use of metallic NPs, particularly Au NPs, to fabricate the imprinted sites, has important implications for future development of sensing devices. The three-dimensional conductivity of the Au NPs provides a means for the electrochemical readout of binding the analyte to the imprinted  $\pi$ -donor sites through the entire sensing surface. The formation of imprinted Au NP clusters may then be used to develop various new optical sensors. Furthermore, the present study used electropolymerization as a method to fabricate the functionalized imprinted Au NPs sensing matrix. Other methods, such as layer-by-layer deposition of Au NPs, may be similarly used to construct imprinted sites for improved sensing.

**Supporting Information Available:** (i) TEM image of the thioaniline-functionalized Au NPs; (ii) redox response of the oligoaniline bridging units, formed upon the electropolymerization of the thioaniline-functionalized Au NPs on the thioaniline-modified Au surface; (iii) analysis of TNT and DNT at a bare Au electrode, and (iv) analysis of variable TNT concentrations in groundwater and seawater samples are described. This material is available free of charge via the Internet at <http://pubs.acs.org>.

**Acknowledgment.** Parts of this research project are supported by the Israel Ministry of Defense. M.R. acknowledges the CAMBR fellowship.

JA711278C

(38) Gao, D.; Zhang, Z.; Wu, M.; Xie, C.; Guan, G.; Wang, D. *J. Am. Chem. Soc.* **2007**, *129*, 7859–7866.

(39) Hu, X.; An, Q.; Li, G.; Tao, S.; Liu, J. *Angew. Chem., Int. Ed.* **2006**, *45*, 8145–8148.